# Photonic Signal Processing of Microwave Signals

Robert A. Minasian, *Fellow, IEEE*

*Invited Paper*

***Abstract*—Photonic signal processing offers the prospect of realizing extremely high multigigahertz sampling frequencies, overcoming inherent electronic limitations. This stems from the intrinsic excellent delay properties of optical delay lines. These processors provide new capabilities for realizing high time-bandwidth operation and high-resolution performance. In-fiber signal processors are inherently compatible with fiber-optic microwave systems and can provide connectivity with built-in signal conditioning. Fundamental principles of photonic signal processing, including sampling, tuning, and noise, are discussed. Structures that can extend the performance of photonic signal processors are presented, including methods for improving the filter shape characteristics of interference mitigation filters, techniques to increase the stopband attenuation of bandpass filters, and methods to achieve large free spectral range. Several photonic signal processors, including high-resolution microwave filters, widely tunable filters, arbitrary waveform generators, and fast signal correlators, are discussed. Techniques to solve the fundamental noise problem in photonic signal processors are described, and coherence-free structures for few-tap notch filters are discussed. Finally, a new concept for realizing multiple-tap coherence-free processor filters, based on a new frequency-shifting technique, is presented. The structure not only eliminates the phase-induced intensity noise limitation, but can also generate a large number of taps to enable the achievement of processors with high performance and high resolution.**

***Index Terms*—Microwave photonics, optical delay lines, optical filters, photonic signal processing.**

## I. INTRODUCTION

SIGNAL processing using optical delay lines is a powerful technique for processing high-bandwidth signals. Photonic signal processing can overcome the inherent bottlenecks caused by limited sampling speeds in conventional electrical signal processors. The attractive and unique delay properties of optical waveguides have spurred the development of novel photonic signal processor structures that can exploit the high time-bandwidth product capabilities of this approach. These new techniques transcend the limitations of existing electronic methods, and enable new structures to be realized, which not only can process high-speed signals but which can also realize highly adaptive and reconfigurable operation.

The use of optical fiber as a delay medium for signal processing applications, which was first proposed by Wilner and van den Heuvel [1] and later developed by some pioneering optical delay-line signal processing work at Stanford University, Stanford, CA [2]–[5], has become an active research area. This is motivated by the ability of photonic signal processing to process high-bandwidth signals and to allow direct processing of high-frequency signals that are already in the optical domain. This opens up new possibilities for the realization of high-resolution wide-band processing of signals contained within the fiber.

The unique functional advantages of photonic signal processors [6], including the inherent speed, parallel signal processing capability, low-loss (independent of RF frequency) delay lines, very high sampling frequency ability (over 100 GHz in comparison to around 1 GHz with electronic technology), and electromagnetic interference (EMI) immunity, have led to diverse applications. Photonic signal processor applications include signal filtering [7], multigigabit per second analog-to-digital (A/D) converters [8], frequency converters and mixers [9], signal correlators [10], arbitrary waveform generators [11], and beamformers for phased arrays [12]. Comprehensive reviews of optoelectronic A/D converters can be found in [13] and [14], and a review of discrete-time incoherent photonic processing techniques can be found in [15].

In this paper, we describe new structures that can extend the performance of photonic signal processors. With reference to the processor transfer function, we present methods for improving the filter shape of microwave photonic filters to realize high-frequency selectivity in interference mitigation filters, techniques to obtain bandpass filters with high stopband attenuation and high skirt selectivity, and methods to realize operation with a large free spectral range (FSR). With reference to the processor noise characteristics, a principal objective of this paper is to address the primary limitation of conventional incoherent processors that arises from the dominant phase-induced intensity noise generation. We propose new coherence-free structures that are founded on generic ideas using time- and frequency-domain concepts, which can eliminate this key noise limitation. A range of photonic signal processors, including high-resolution microwave filtering, widely tunable filters, arbitrary waveform generators, fast and adaptive signal correlators, and coherence-free processor structures, are discussed.

Photonic signal processor applications primarily arise in defense and radioastronomy areas for tackling the problems of processing wide-band fiber-fed distributed antenna signals and for providing essential EMI immunity. In microwave fiber-optic systems that are used for RF antenna remoting and signal routing, the signal is already in the optical domain, hence it is attractive to

Manuscript received June 1, 2005; revised September 2, 2005. This work was supported by the Australian Research Council.

The author is with the School of Electrical and Information Engineering, University of Sydney, Sydney, N.S.W. 2006, Australia (e-mail: r.minasian@ee.usyd.edu.au).

Digital Object Identifier 10.1109/TMTT.2005.863060

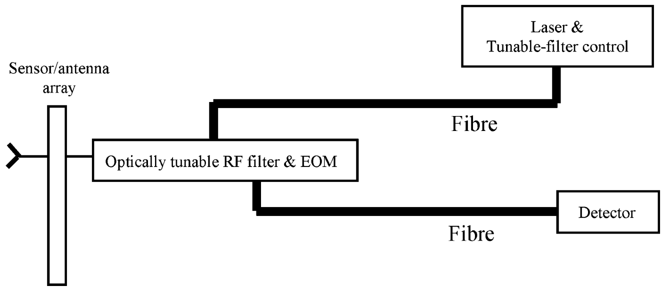


Fig. 1. Front-end architecture providing broadly optically tunable front-end RF filters combined with fiber-fed distributed RF antenna remoting.

also process the signal directly in the optical domain. Specific examples include RF preprocessing and filtering. Other application areas for photonic signal processing occur in the high-frequency regime, where electronic digital signal processing has limited usefulness, and in applications that require very wide-band octave and multioctave tunability. In these applications, photonic signal processing can provide unique solutions that are based on its key capabilities for parallel processing using wavelength-division multiplexing (WDM) techniques.

An example in real-time processing of broad-band radar signals is shown in Fig. 1. In radar applications, multioctave systems suffer from harmonics and other unwanted signals, and RF tunable filters at the front-end are mandatory to eliminate unwanted signals and to reduce A/D converter spurious effects [16]. This is not an easy task for RF technology, and electronic approaches severely limit the performance of multifunction antennas [16]. Optically implemented RF tunable filters have the potential to solve the problems of multioctave microwave operation, have the ability to offer high instantaneous bandwidth and widely tunable range, and can provide the extra important benefits of optical control that enable remoting with no wires. Fig. 1 shows an optical front-end architecture [16] that can provide broadly tunable front-end RF filters and which is combined with the RF antenna remoting.

In the radioastronomy field, the ability to simultaneously excise a very narrow RF interference band from a signal carried in an optical fiber and at the same time to transmit the wanted signal with minimal impact on the information over a wide range of microwave frequencies is required to suppress unwanted manmade signals from terrestrial transmitters and satellites that are picked up by the antenna arrays. These interfering signals, which coexist and are often at much higher levels than the weak desired signals, can easily dominate over the desired signal to make its detection extremely difficult, because they induce nonlinear distortion at the receiver. Conventional optical links [17] do not selectively reject the unwanted interfering signals that may be present with the microwave signals being transmitted. This can severely limit the performance of the complete system, and a major future challenge is the development of new optical microwave transport systems that also have in-built signal conditioning.

A wide range of photonic signal processor filter structures have been reported, based on the optical delay-line concept [18]–[36]. However, most of these structures are subject to a central problem arising from coherence limitations. To obtain a robust transfer characteristic irrespective of environmental perturbations, conventional approaches have required the use of an incoherent approach, in which the coherence time of the light source is made smaller than the minimum delay time of the processor. This inherently imposes a fundamental limitation because the optical interference that occurs in summing the multiple delayed optical signals produces excessive amounts of phase-induced intensity noise (PIIN) at the output. This phase noise is a significant problem [37]–[40], as it is, by far, the dominant noise source and is the major limitation to processor SNR. The coherence issue is the most important issue that limits photonic signal processors. This paper describes recent new methods that can solve this fundamental problem in photonic signal processors. Techniques that provide coherence-free structures for few-tap notch filters are discussed. We also present a new concept for realizing multiple-tap coherence-free processor filters based on a new frequency-shifting technique. This not only eliminates the PIIN limitation, but can also generate a large number of taps to enable the realization of high-resolution processors. This opens the way for realizing high-performance signal processing directly inside the fiber.

This paper is structured as follows. The fundamental principles of photonic signal processing, including basic operation, generic requirements, delay media, and sampling, are presented in Section II. Techniques for tuning the processor function to obtain reconfigurable operation for both continuous tuning and discrete digital tuning are described in Section III. Key noise issues in conventional photonic signal processors operating in the incoherent regime that arise from PIIN are discussed in Section IV. Methods for improving the filter shape of microwave photonic filters to realize high-frequency selectivity in interference mitigation filters at microwave frequencies, for bandpass filters with high stopband attenuation and high skirt selectivity, and for operation with a large FSR are described in Section V. The use of sampling and discrete-time processor techniques to synthesise high-speed arbitrary waveforms using photonics is discussed in Section VI. Grating-based processors that can perform high-speed correlation of signals for programmable optical code correlation are described in Section VII. Finally, Section VIII discusses photonic signal processor structures that can resolve the problem of eliminating PIIN limitations and presents a new concept for realizing multiple-tap coherence-free processors which can operate without phase noise limitations and which can generate a large number of taps to realize high-resolution processors.

## II. PRINCIPLES OF PHOTONIC SIGNAL PROCESSING

The fundamental discrete-time signal processor has a structure in which successive samples of the signal are delayed, weighted, and summed. For an input signal denoted by $x(t)$, the output is given by

$$y(t) = \sum_{n=0}^{N} W_n x(t - nT) \tag{1}$$

where $W_n$ is the $n$th tap weight, $N$ is the number of taps, and $T$ is the sampling period. If the impulse response has only a finite number of nonzero samples, this is defined as a finite-impulse response (FIR) system, which is a characteristic of nonrecursive filters. If the impulse response has an infinite number of terms,

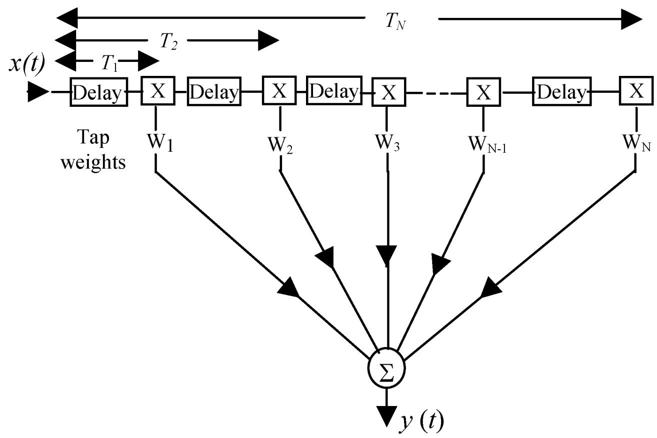


Fig. 2. Basic delay-line processor structure.

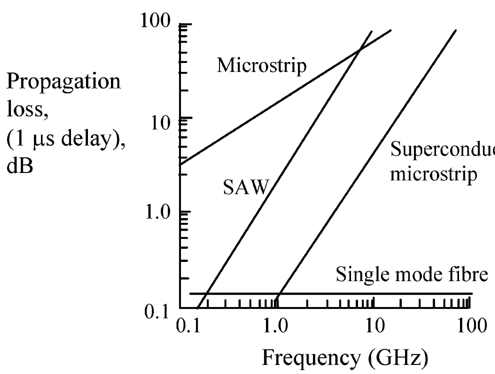


Fig. 3. Propagation loss characteristics of various delay media.

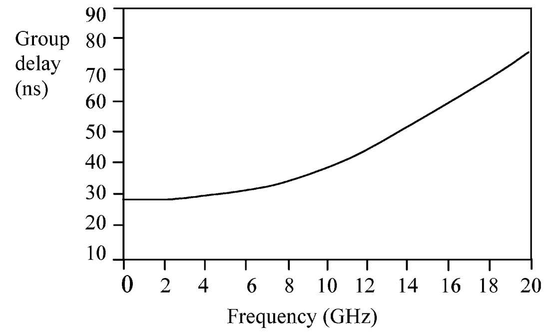


Fig. 4. Group delay for a superconducting YBCO thin-film microstrip delay line [41].

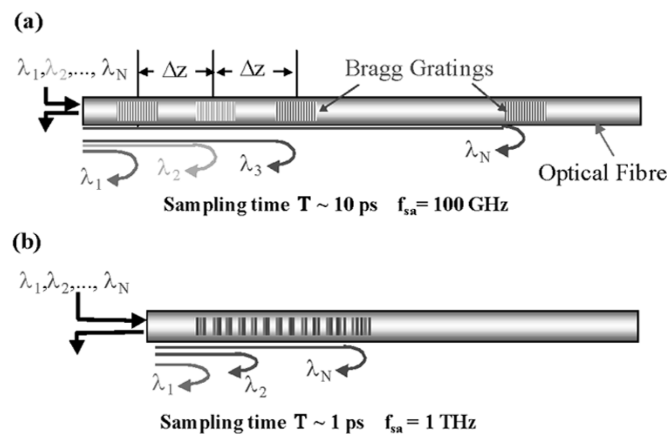


Fig. 5. High-speed sampling techniques using grating elements. (a) Discrete grating arrays. (b) Superposed arrays.

this is referred to as an infinite-impulse response (IIR) system, which is a characteristic of recursive filters. These structures can generate a wide variety of signal processing functions. In addition, by programming either the tap weights or the unit delay time, adaptive processing can be obtained. The basic delay-line structure is shown in Fig. 2. This provides a discrete-time approximation to a desired impulse response.

Generic requirements of photonic signal processors include the generation of many taps in order to increase the resolution in the frequency domain and the ability to obtain short sampling periods to increase the resolution in the time domain.

The fundamental functions of a signal processor, namely: 1) sampling; 2) multiplication (amplitude weighting); 3) time delay; and 4) addition can be achieved in a variety of ways. The unique advantages of optical delay lines relative to other delay-line media can be seen in Figs. 3 and 4. The propagation loss characteristics of various delay media, including surface acoustic wave (SAW) delay lines, microstrip, superconducting delay lines, and optical fiber are shown in Fig. 3. The key feature of the optical delay medium is that the loss is independent of the modulating frequency for frequencies well into the microwave and millimeter-wave frequency range. None of the other delay media exhibit this characteristic. A secondary benefit is that the loss of optical delay is significantly lower than that of other delay media for a comparable delay time. Another important advantage can be noted by examining the group delay characteristics of the delay media. Alternative approaches, such as implementing the delay line directly using microwave media, suffer from significant group delay variations, as shown in Fig. 4 for a recently reported superconducting YBCO thin-film microstrip delay line (at a temperature of 30 K) [41] over the frequency range to 20 GHz. By contrast, the dispersion of optical fiber is extremely low and is controllable. The intrinsic reason why the optical medium exhibits these excellent, essentially frequency-independent characteristics for delay-line applications is that the fractional bandwidth for optical delay lines is negligible. This also holds for the multiplication/amplitude weighting operation, where optical couplers, for instance, can provide frequency-independent RF signal weighting to extremely high frequencies, since the fractional bandwidth for the coupling ratio is insignificant. These fundamental factors give optical delay media intrinsic advantages, which have spurred the development of photonic signal processing.

The sampling operation can be implemented in a variety of ways including unbalanced Mach–Zehnder structures [25], [26], and arrayed waveguides (AWGs) [27]. Bragg gratings are particularly attractive as sampling elements, because they enable the tap weights to be controlled via the grating reflectivity, the sampling time to be controlled via the grating spacing, and the interaction wavelength to be controlled via the grating pitch. The latter is a particularly powerful feature, which together with WDM provides one of the most promising approaches for creating high-capacity signal processors. Fig. 5 shows several fiber-based sampling techniques.

The processor sampling frequency is determined by the minimum delay step size. The processor sampling frequency is given by

$$f_{\mathrm{sa}} = \frac{1}{T}. \tag{2}$$

Extremely high sampling frequencies can be realized through the use of grating elements. A discrete fiber Bragg grating (FBG) array for time delay processing of signals is shown in Fig. 5(a). For high reflectivity, the minimum practical center-to-center grating spacing is around 1 mm, resulting in a minimum delay step size of 10 ps [42]. This corresponds to a sampling frequency of 100 GHz.

Superposed fiber gratings [see Fig. 5(b)] based on multiple overwritten gratings with different Bragg wavelengths in the same length of fiber can realize even smaller delay increments [43].

The effective reflection point for each wavelength is controlled by selecting a different coupling coefficient for each individual superposed grating. Superposed grating designs have been shown to be capable of realizing 32 time delay steps at 1-nm wavelength spacing with a 1-ps delay increment. This delay step corresponds to a sampling frequency of 1 THz.

## III. Tunable Processors and Reconfigurable Functions

As well as its ability to operate at high speed, another principal advantage of photonic signal processing over electronic signal processing is its ability to realize extremely wide tunability in the processor function. Whilst varactor and varactor MEMs enable continuous frequency tuning over a range of several percent and recently reported MEMs switches enable digital discrete frequency tuning in the 40% range [44], [45], photonic signal processing techniques enable tuning of octaves or even decades of continuous tuning range. The ability to achieve a wide tuning range is important especially for future reconfigurable RF front-ends for radar systems.

A widely used and basic principle for tuning the photonic signal processor function is shown in Fig. 6. In this structure, the basic time delay can be controlled in either a continuous manner, as shown in Fig. 6(a), or a discrete digital method, as shown in Fig. 6(b).

By changing the wavelength of the optical source over the chirp range of the fiber grating or across the grating array, the point of reflection along the length is shifted, and, hence, the basic time delay of the processor can be controlled and hence the filter frequency can be tuned. Wavelength tuning can be fast, and this permits agile programming capability. This results in continuously variable and widely tunable processors.

## IV. Noise

The most important noise source in photonic signal processors operating in the incoherent regime arises from PIIN. To obtain a robust transfer characteristic irrespective of environmental perturbations, conventional approaches have required the use of an incoherent approach, such that the coherence time of the light source is smaller than the minimum delay time of the processor. This in turn means that the laser linewidth is larger than

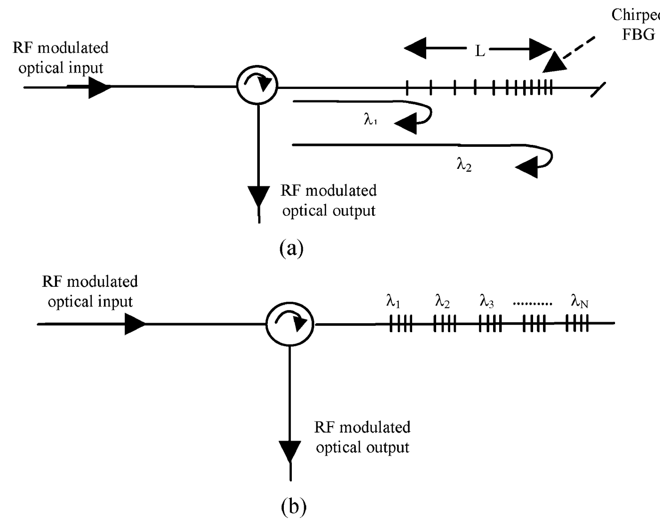


Fig. 6. Basic principle for tuning the photonic signal processor function.

the processor FSR. The linewidth of the laser manifests itself in random phase variations of the optical output with time. In photonic signal processors, the laser power is tapped into different paths and is recombined at the output. The summation of the multiple delayed optical signals at the square-law photodetector causes conversion of the laser phase fluctuations into intensity fluctuation noise (PIIN) at the output.

For a given optical source, the number of optical taps and the weights of these taps that are combined determine the spectrum and level of the PIIN. For a given processor structure, the PIIN is also related to the coherence time of the optical source. Hence, the spectrum of the PIIN is a function of the topology of the processor and the coherence of the optical source.

PIIN noise is normally the dominant noise source in incoherent photonic signal processors, and hence it is important to understand its characteristics. PIIN noise has been analyzed in [37] and [38]. This provides a general formulation that applies for arbitrary coherence optical sources, including both incoherent and coherent cases, and which is based on the amplitude and phase of the delayed signals, which makes it applicable to any delay-line structure.

Since photonic signal processing structures are linear time-invariant discrete systems, the system can be characterized by its response to an input field amplitude response. The complex field amplitude impulse response $\vec{h}(t)$ can be expressed as

$$\vec{h}(t) = \sum_{n=0}^{N} \vec{h}_n \delta(t - nT) \tag{3}$$

where $N$ is the number of taps produced by the signal processor, $\vec{h}_n$ represents the complex amplitude of impulse at the time $t = nT$, and $T$ is the time delay between each tap. Expressing the optical source electric field as

$$\vec{E}_{\mathrm{in}}(t) = \sqrt{I_0} e^{j(\omega_0 t + \phi(t))} \tag{4}$$

where $I_o$ is the average output laser power, $\omega_o$ is the central angular optical frequency, and $\phi(t)$ is the time-varying random laser phase of the light that determines its linewidth and coherence, the output electric field of the delay line processor is given by the convolution

$$\vec{E}_{\text{out}}(t) = \vec{h}(t) * \vec{E}_{\text{in}}(t). \tag{5}$$

Thus,

$$\vec{E}_{\text{out}}(t) = \sum_{n=0}^{N} \vec{h}_n \vec{E}_{\text{in}}(t - nT). \tag{6}$$

The photocurrent is proportional to optical intensity and can be expressed as

$$\begin{aligned} I(t) &= |\vec{E}_{\text{out}}(t)|^2 \\ &= \sum_{n=0}^{N} \sum_{m=0}^{N} \vec{h}_n \vec{h}_m^* \vec{E}_{\text{in}}(t - nT) \vec{E}_{\text{in}}^*(t - mT) \end{aligned} \tag{7}$$

where $*$ denotes complex conjugation. Using the Wiener–Khinchine theorem, the spectrum of the photocurrent is the Fourier transform of the autocovariance function of $I(t)$. The autocovariance function is given by subtracting the average light intensities from the total intensities

$$\text{cov}(t_1, t_2) = \langle I(t_2) I(t_1) \rangle - \langle I(t_2) \rangle \langle I(t_1) \rangle. \tag{8}$$

Combining (4) and (7) yields

$$\begin{aligned} &\langle I(t_2) I(t_1) \rangle \\ &= I_o^2 \sum_{n_1=0}^{N} \sum_{n_2=0}^{N} \sum_{m_1=0}^{N} \sum_{m_2=0}^{N} \vec{h}_{n_1} \vec{h}_{m_1}^* \vec{h}_{n_2} \vec{h}_{m_2}^* \\ &\quad \times e^{j[\omega_0 (m_1 - n_1 + m_2 - n_2) T]} \\ &\quad \times \left\langle e^{j[\phi[t_2 - n_1 T) + \phi(t_1 - n_2 T) - \phi(t_2 - m_1 T) - \phi(t_1 - m_2 T)]} \right\rangle \end{aligned} \tag{9}$$

and in a similar manner

$$\begin{aligned} \langle I(t_2) \rangle \langle I(t_1) \rangle = &I_o^2 \sum_{n_1=0}^{N} \sum_{n_2=0}^{N} \sum_{m_1=0}^{N} \sum_{m_2=0}^{N} \vec{h}_{n_1} \vec{h}_{m_1}^* \vec{h}_{n_2} \vec{h}_{m_2}^* \\ &\times e^{j[\omega_0 (m_1 - n_1 + m_2 - n_2) T]} \\ &\times \left\langle e^{j[\phi[t_2 - n_1 T) + \phi(t_2 - m_1 T)]} \right\rangle \\ &\times \left\langle e^{j[\phi[t_1 - n_2 T) - \phi(t_1 - m_2 T)]} \right\rangle. \end{aligned} \tag{10}$$

The time-varying phase fluctuation of the laser light is usually assumed to undergo a random-walk process and is statistically modeled as a Wiener–Levy random process [46], with a structure function

$$D_\phi(t_a, t_b) = \langle [\phi(t_a) - \phi(t_b)]^2 \rangle \tag{11}$$

where $t_a$ and $t_b$ are two arbitrary time instants and $D_\phi(t_a, t_b)$ is the variance of the phase difference.

The autocovariance function is given by

$$\begin{aligned} \text{cov}(t_1, t_2) = &I_o^2 \sum_{n_1=0}^{N} \sum_{n_2=0}^{N} \sum_{m_1=0}^{N} \sum_{m_2=0}^{N} \vec{h}_{n_1} \vec{h}_{m_1}^* \vec{h}_{n_2} \vec{h}_{m_2}^* \\ &\times e^{j[\omega_0 (m_1 - n_1 + m_2 - n_2) T]} e^{-\frac{1}{2} D_{\Delta\phi}(n_1, m_1, n_2, m_2, \tau)} \end{aligned} \tag{12}$$

where

$$\begin{aligned} &D_{\Delta\phi}(n_1, m_1, n_2, m_2, \tau) \\ &\quad = D_\phi[|(m_1 - n_1)T|] + D_\phi[|(m_2 - n_2)T|] \\ &\qquad + D_\phi[\tau + |(m_2 - n_1)T|] + D_\phi[\tau + |(n_2 - m_1)T|] \\ &\qquad - D_\phi[\tau + |(n_2 - n_1)T|] - D_\phi[\tau + |(m_2 - m_1)T|] \end{aligned} \tag{13}$$

and $\tau = t_1 - t_2$.

For the case where the system is operating in the incoherent region $\tau_c \ll T$ (where $\tau_c$ is the optical source coherence time) and the laser lineshape behaves as a Lorentzian function, the autocovariance function can be expressed as

$$\begin{aligned} \text{cov}(\tau) = 2I_0^2 \sum_{l=1}^{N} &\left[ \sum_{k=-(N-1)}^{N-1} \text{Re}[G_{0,1}(|k|) \delta(\tau - kT)] \right] \\ &* e^{-|\tau|/\tau_c} \end{aligned} \tag{14}$$

and

$$\begin{aligned} G_{0,l}(|k|) = &\sum_{i=0}^{N-|k|-l} \vec{h}_{i+l} \vec{h}_i \vec{h}_{i+|k|+l} \vec{h}_{i+|k|} \\ &\times e^{j(\phi_{i+l} - \phi_i - \phi_{i+|k|+l} + \phi_{i+|k|})} \end{aligned} \tag{15}$$

where $h_i$ and $\phi_i$ are the amplitude and phase of the $i$th tap.

The PIIN noise power spectral density is given by the Fourier transform of (14) to yield

$$\begin{aligned} S(f) = 2I_0^2 \sum_{l=1}^{N} &\left[ \text{Re}[G_{0,l}(0)] + 2 \sum_{k=1}^{N-1} \text{Re}[G_{0,l}(k)] \cos(2\pi kTf) \right] \\ &\times \frac{2\tau_c}{1 + (2\pi f \tau_c)^2}. \end{aligned} \tag{16}$$

Equation (16) reveals that there are two separate effects that contribute to PIIN. The first term is the impulse summation term $S_\delta(f)$

$$S_\delta(f) = \sum_{l-1}^{N} \text{Re}[G_{0,l}(0)] + 2 \sum_{l=1}^{N} \sum_{k=1}^{N-1} \text{Re}[G_{0,l}(k)] \cos[2\pi kTf] \tag{17}$$

which only depends on the processor configuration and is a function of the topology of the delay-line structure. The second term only depends on the optical source and is related to the optical source coherence $\tau_c$. Equation (16) is applicable to both recursive and nonrecursive delay-line structures. An example of its evaluation for a recirculating delay-line structure can be found in [37] and [47].

It can be seen that the impulse summation term $S_\delta(f)$ has a $\cos[2\pi kTf]$ term, which can be interpreted as resulting in harmonic components of the noise spectrum. This produces periodic peaks or notches in the noise spectrum at harmonics of $1/T$, where $T$ is the tap delay. Examining (17) for $S_\delta(f)$ in more detail reveals that it involves summation over the range of $N$, where $N$ is the number of taps in the processor response. Hence, in general, the $S_\delta(f)$ spectrum level increases as the number of taps generated by the photonic signal processor increases. This is significant, because high-resolution processors require a large

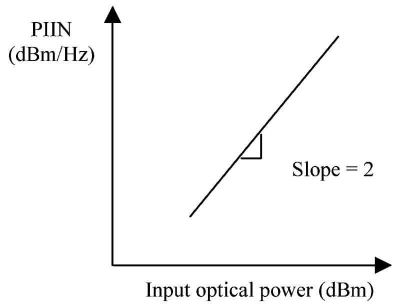


Fig. 7. Dependence of the PIIN spectral density on the laser optical power.

number of taps, and, thus, efforts to increase the resolution of the processor are accompanied by an increase in PIIN.

The dependence of the PIIN spectral density on the laser optical power is given from (16) as

$$S(f) \propto I_0^2 \tag{18}$$

which reveals that the PIIN increases with the square of the laser input power, as shown in Fig. 7.

Since the RF signal also increases with the square of the laser power, this means that the SNR of the processor cannot be increased by increasing the input optical power when PIIN is dominant, which is the usual case.

The performance of the photonic signal processor is affected by several noise sources, including shot noise, laser relative intensity noise, receiver electronic noise, and PIIN. Typically, the PIIN is several orders of magnitude larger than the other noise sources. Thus, PIIN noise, by far, dominates the noise in the system and constitutes the most significant degradation to the SNR of the processor. The SNR can be improved by increasing the signal modulation index or by decreasing the PIIN spectral density. Techniques to achieve the latter include modifying the laser lineshape [48], [49], using balanced detection to suppress the noise, or selecting a structure that minimizes the impulse summation term. However, these approaches give limited improvement. Novel techniques that can resolve the problem of eliminating the PIIN are described in Section VIII.

## V. Microwave Photonic Filters

Principal objectives for microwave photonic filters include the realization of high-frequency selectivity at microwave frequencies, high stopband attenuation, high skirt selectivity, and operation with a large FSR. Methods for improving the filter shape of microwave photonic filters to realize high-frequency selectivity in interference mitigation filters, for obtaining high stopband attenuation and high skirt selectivity in bandpass filters, and for increasing the FSR are described in this section.

### A. Interference Mitigation Filters

The antenna, in radar or fiber radio systems, typically receives unwanted high-amplitude interfering signals in addition to the wanted signal. The former must be rejected to avoid undue demands on the dynamic range requirements of the fiber-optic link. A photonic signal processor can excise the interference in the fiber signal by providing a narrow stopband, while simultaneously transmitting the wanted signal over a flat wide passband. A general topology for a fiber-based interference mitigation filter that can realize this function is shown in Fig. 8.

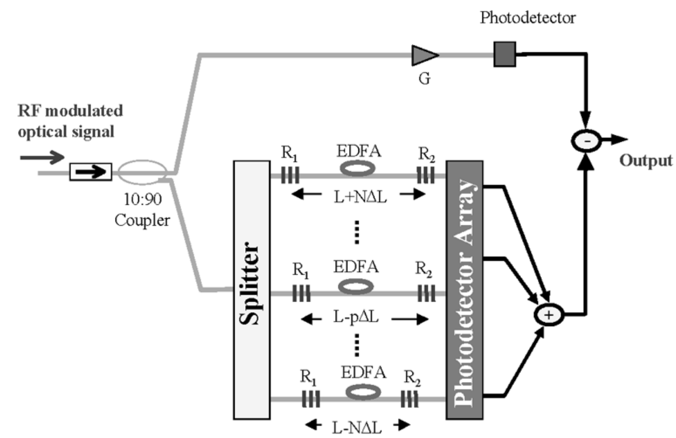


Fig. 8. Fiber-based filter for interference mitigation.

The squareness of the filter stopband response (or shape factor, which is defined as the ratio of the $-3$-dB bandwidth to the $-40$-dB bandwidth) is important. A low shape factor is essential for interference mitigation filters so that the interference band is fully excised, but there is minimal impact on the passband. This becomes more difficult to achieve the narrower the stopband becomes, because it implies that very steep transition edges around a narrow high-suppression stopband region are required.

The structure in Fig. 8 solves this problem by introducing a multiple cavity with noncommensurate delay lines in the topology. The concept uses multiple photonic bandpass filters. These $N$ photonic filters are designed to be slightly detuned from the center frequency corresponding to the required notch frequency $f_o$ and are operated at frequencies $f_o - n\Delta f$ and at $f_o + n\Delta f, n = 1, 2, \ldots, N$. This is shown by the offset cavity lengths between the Bragg gratings of $L+n\Delta L$ and $L-n\Delta L$ in Fig. 8, which form the noncommensurate delay-line approach. The bandpass filter frequencies are slightly detuned from the fundamental frequency of the notch processor, so the combined response of the bandpass filters yields a squarer response. This combined response is subtracted from the all-pass direct path response, to give a narrow-stopband filter response, with very flat and wide passbands around it.

In this structure, the active cavities introduce different poles. The position of each pole is principally controlled by the difference in cavity length and by the erbium-doped fiber amplifier (EDFA) gain and the reflectivities of the Bragg gratings $R_1$ and $R_2$. The zero corresponds to a notch frequency $f_0 = 1/T = c/(2nL)$, where $T$ is the round-trip delay time corresponding to a cavity length $L$, $n$ is the fiber refractive index, and $c$ is the speed of light. The 3-dB bandwidth of the notch filter is mainly controlled by the cavity length difference and the EDFA gain. To increase the squareness of the stopband, it is required that the poles of the bandpass filters are close to one another, so that their combined response gives a flat top with steep edges. This ensures that the notch filter stopband is wider than that of the single cavity, while still producing negligible effect on the flatness of the passband response of the overall filter. The length offset $2p\Delta L$ between the active cavities adjusts the shape factor

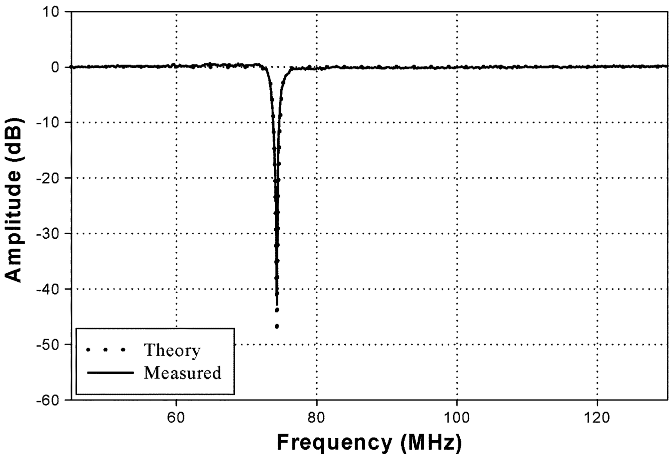


Fig. 9. Frequency response of the fiber-based interference rejection filter for the simple case comprising a dual cavity.

of the filter and can be optimized to obtain the minimum shape factor.

The general structure shown in Fig. 8 requires a number of EDFAs, which increases the relative complexity for its implementation. Note, however, that only a very low gain (typically around 1.97) is required for the EDFAs, and, hence, a single pump can be used with a splitter to pump all of the EDFAs. Since the pump is the most expensive part of the system, this constrains the overall expense. Nevertheless, the number of line sections that are used will involve a tradeoff between complexity and filter response performance.

Fig. 9 shows an example of the frequency response of this fiber-based interference rejection filter for the simple case comprising a dual cavity [7]. The experimental results are at relatively low frequencies for ease of measurement. In this case, fiber cavity lengths were 1.4 m, and the length offset between the two cavities was 2 cm. The results exhibit an extremely flat response in the passband, together with a large reduction in the shape factor of the rejection band, to provide high-resolution interference mitigation. This structure can be extended to higher frequencies by reducing the lengths of the cavities. This can be achieved using fiber-based cavities; however, at very high frequencies, the required length accuracy will become a limitation. At very high frequencies, the best approach is to implement the structure using planar lightwave circuit technology, which can define the lengths with high precision.

### *B. High-Skirt-Selectivity Bandpass Filters*

Another requirement for signal conditioning in optical transport systems is the ability to select wanted signals with high-resolution bandpass filtering but to reject adjacent unwanted frequencies. Several photonic bandpass filters [18]–[25], [31]–[33] have shown high-$Q$ frequency responses, however, they have limited stopband rejection and skirt selectivity. This is because of the constraints of the topologies, which restrict the possible pole-zero placements and which cause a gradual response fall-off in the attenuation regions, so that even far away from the filter center frequency it is not possible to obtain large stopband attenuation. High stopband attenuation and skirt selectivity are essential to ensure that a high rejection of unwanted frequencies adjacent to the desired signal frequency is obtained.

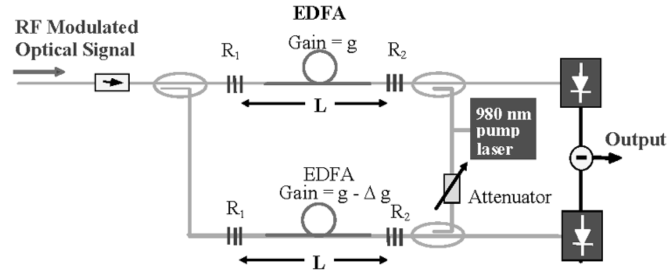


Fig. 10. Structure of the dual-cavity parallel topology fiber-based bandpass filter.

Fig. 10 shows a concept based on offset gain cavities, which solves the problem of realizing high-$Q$ bandpass filters with high skirt selectivity. This is based on a dual-cavity optical structure in which two pairs of active FBG cavities are used with optical gain offset to control the poles and filter stopband attenuation characteristics. This can cancel the wide pedestal regions of the response away from the center frequency to enable a large improvement in stopband attenuation and skirt selectivity. Again, only a single pump is needed with a splitter to pump both the EDFAs that operate with very low gain.

The concept here is to split the modulated signal equally, using a 50 : 50 coupler, into two paths and to introduce two cavities that are designed to operate as bandpass filters at the same center frequency, but which operate with a small gain offset. The upper arm has a gain of $g$, while the lower arm has a gain of $g - \Delta g$. The gain offset $\Delta g$ is controlled by the optical attenuator, which adjusts the pump power launched in the lower cavity. This offset causes the upper arm bandpass filter to have a higher optical gain and hence a sharper response around the center frequency than the lower arm bandpass filter, however, far away from the center frequency the responses of both arms are nearly identical. Thus, the contrast in the characteristics between the top and bottom filters is significant near their center frequency, however the contrast is negligible elsewhere. Each output is detected using a photodiode in a balanced configuration so as to subtract the photocurrents. This produces a sharp response near the filter center frequency and cancels the output at the out-of-band frequencies. Hence, the output results in a response that is slightly sharper around the center frequency than the single-arm response alone, but most importantly the wide pedestal region far away from the center frequency is nearly cancelled out [50]. The stopband attenuation can exceed 60 dB over 1.5 times the FSR. This offset-gain structure enables the realization of high stopband attenuation and skirt selectivity to attain high rejection of unwanted frequencies adjacent to the desired signal frequency.

### *C. Filters With High FSR*

The recursive nature of discrete-time signal processors limits the realizable width of the useful frequency range because unwanted additional periodic responses come into effect at higher frequencies. To increase the filter useful operational bandwidth, it is essential to suppress the recursive responses.

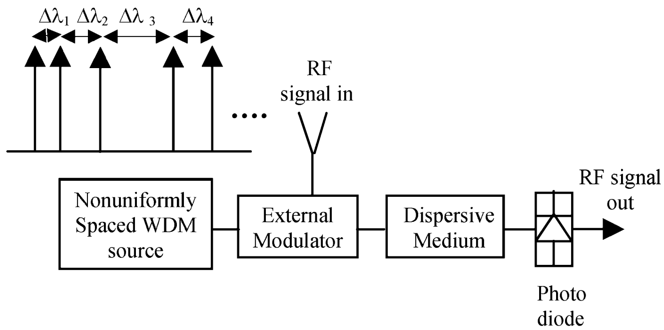


Fig. 11. Harmonic suppressed photonic microwave bandpass filter based on nonuniform tap spacing [51].

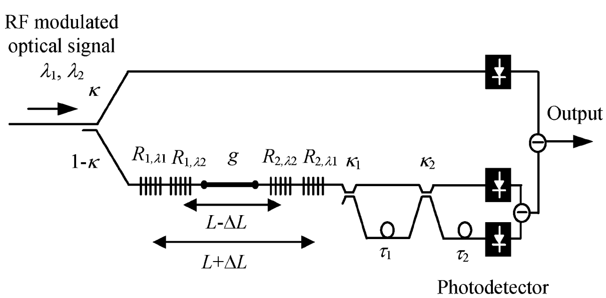


Fig. 12. Structure of the large FSR filter microwave photonic notch filter.

A technique for achieving this for bandpass filters is shown in Fig. 11 [51]. This is based on using a nonuniform wavelength spacing between optical carriers. Using an appropriate nonuniform spacing distribution, the spectral filter transfer function becomes the product of two uniformly spaced transversal filters but with different FSR values. By means of the Vernier principle, the overall resultant FSR can be made larger, thus increasing the filter rejection bandwidth.

A different technique that can overcome this limitation for a photonic notch filter [52] to give a multifold increase in the FSR is shown in Fig. 12.

This is based on using multiple wavelengths and grating-based cavities centered at the different wavelengths to realize a dual-cavity noncommensurate delay-line bandpass filter [7]. The natural periodic response of the notch filter is suppressed by the delay-line structure following the WDM grating cavities [52]. This comprises a cascade of unbalanced delay lines that have delay differences $\tau_1$ and $\tau_2$, which introduce a series of notches that suppress several harmonic responses of the multiple-wavelength bandpass filter. Hence, after subtraction of the combined signal from the all-pass arm, the desired notch at $f_0$ is realized; however, the potential notches at several harmonics are suppressed, and the passband is significantly extended.

Fig. 13 shows the response for this structure, which exhibits a notch bandwidth of 1% of center frequency and a passband FSR increase by a factor of 4, demonstrating the ability of producing both a square-type notch response and a large FSR notch filter response.

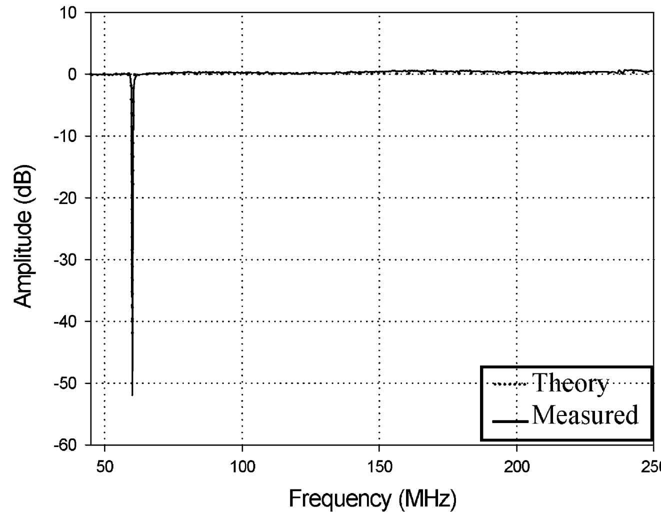


Fig. 13. Large FSR notch filter frequency response.

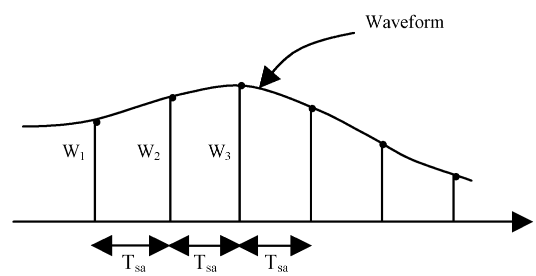


Fig. 14. Arbitrary waveform to be generated, together with its samples at the sampling intervals $T_{\mathrm{sa}}$.

## VI. Arbitrary Waveform Generation Using Photonic Processing

The synthesis of high-speed arbitrary waveforms using photonics has applications in radar, signal processing, and communications. Photonic techniques have potential advantages in overcoming electronics-based limitations in generating high-frequency waveforms and achieving the very high sampling frequencies required and in overcoming the limited speed and linearity of electronic device technology such as digital-to-analog converters. Photonics-based waveform generator approaches include spectral shaping of a supercontinuum pulse [53], phase-locked longitudinal modes, and Fourier synthesis using independent lasers [54].

A different photonic method for generating high-speed arbitrary RF waveforms, based on a sampling and delay-line technique, is shown in Fig. 14. The waveform to be generated is shown, together with its samples at the sampling intervals $T_{\mathrm{sa}}$. The sampling and weighting operation can be identified to be similar to the function expressed in (1). Hence, discrete-time photonic processing techniques can be used to implement the synthesis of the waveform.

Fig. 15 shows how this concept can be realized. It is based on the generation of short sample pulses using photonics, the generation of high sampling rates using short delay steps in fiber grating reflectors in conjunction with a delay-line structure, and the generation of arbitrary high-speed waveforms using sample weighting and filtering.

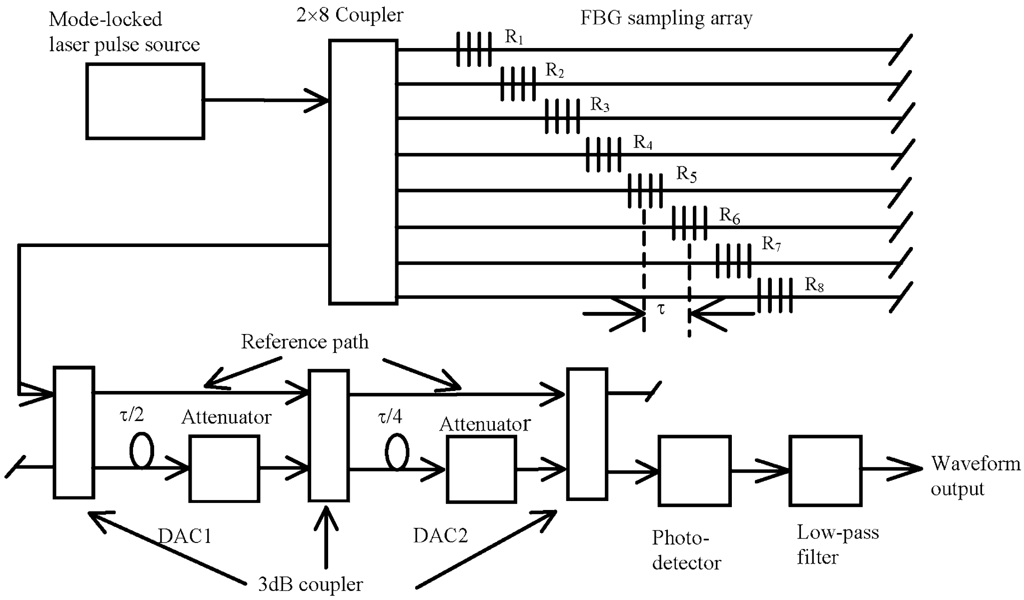


Fig. 15. Structure of the photonic waveform generator.

The short optical pulse is reflected off an array of $N$ FBGs, whose locations give sequential delays to create the sampling time and whose reflectivities are designed so that a series of weighted pulses are returned to the output to create the sample amplitudes [55]. This effectively provides controllable samples of the required arbitrary waveform. Since the difference in the grating positions can be made very small, extremely high sampling frequencies can be obtained. To increase the number of samples, the signals reflected off of the FBGs are fed into a concatenated series of 50 : 50 couplers whose outputs comprise a reference path and a processing path with a delay in time and attenuation in amplitude. The splitting of the generated pulse train into two paths at each coupler, one of which is delayed and attenuated relative to the other, enables the interleaving and the insertion of intermediate pulses, before summing the output of the two paths to obtain an effective doubling in the number of pulses generated at each stage. The large exponential increase in the number of pulses that can be generated by cascading the delay and attenuation stages is an important feature of this structure. It enables an effective increase in the number of samples to be generated for synthesizing waveforms with fast transitions, which contain high-order Fourier frequency components in the waveform, as required by the Nyquist criterion.

## VII. Signal Correlators

Grating-based processors can perform high-speed correlation of signals. Fig. 16 shows a structure for an all-optical correlator using FBG arrays as tunable elements for programmable optical code correlation [56]. This provides a simple technique for programming the code recognition and for reconfiguration of the correlator function by piezoelectric tuning of the Bragg wavelength.

For an $n$-grating array, $2^n$ different codes can be processed by this correlator. The output is given by

$$R(\tau) = \int_{-\infty}^{\infty} s(t) f(t-\tau)\, dt \tag{19}$$

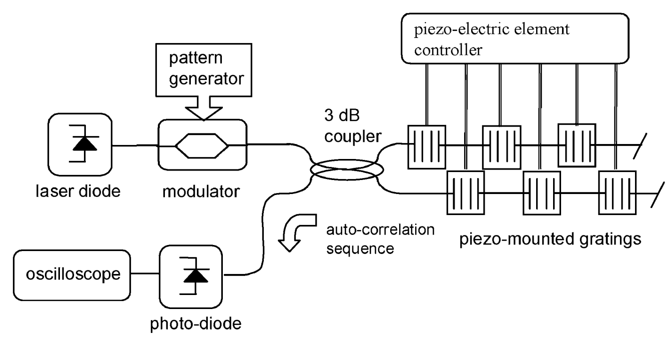


Fig. 16. Programmable grating-based signal correlator.

where $s(t)$ represents the incoming code sequence and $f(t)$ represents the stored impulse response. Autocorrelation output is obtained only if the two bit sequences $f(t)$ and $s(t)$ are identical. This correlator has the ability to decode ultrafast sequences at multigigabit per second rates and can be programmed to recognize different high bit-rate codes by tuning the gratings.

## VIII. Photonic Signal Processors Without Phase-Noise Limitations

The significance of the phase-noise problem in incoherent photonic signal processors has been discussed in Section IV. The PIIN noise, by far, dominates the noise in such systems and constitutes the most significant problem that can severely degrade the SNR of the processor. Hence, it is important to address photonic signal processor structures that can resolve the issue of eliminating phase noise, to open the way for realizing high-performance, wide-band, and adaptive signal processing directly inside the fiber.

### A. WDM Photonic Signal Processors

The most straightforward means of eliminating coherence limitations in photonic signal processors is to use a multiple-wavelength WDM delay-line technique [57]. The WDM implementation of such an approach with a laser array of $N$ elements

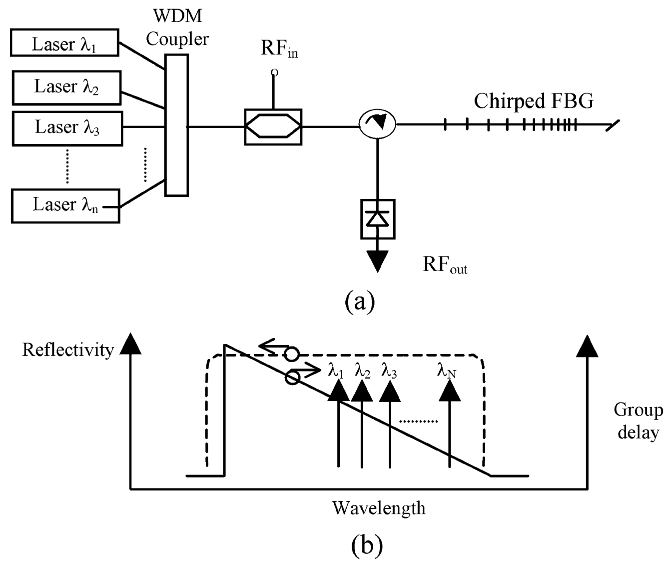


Fig. 17. Layout of filter with a laser array of $N$ elements and a linearly chirped fiber grating [58].

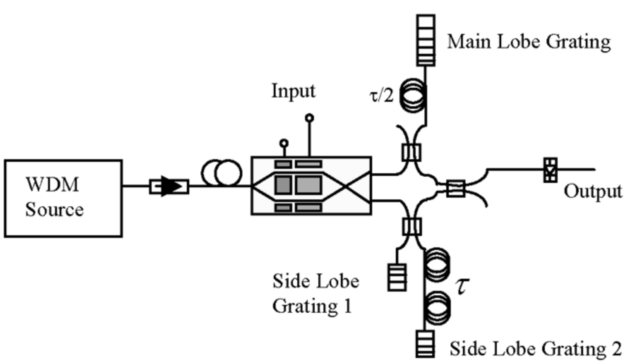


Fig. 18. Grating synthesized photonic filter structure.

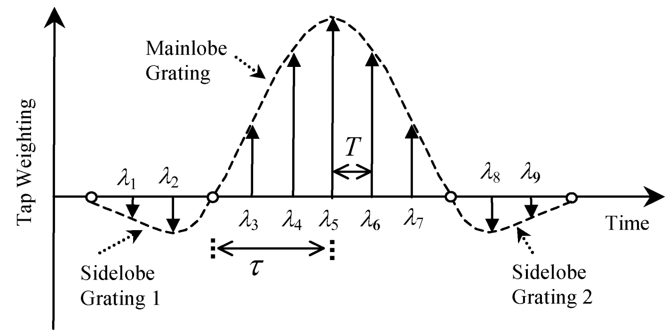


Fig. 19. Impulse response of the grating synthesized photonic filter.

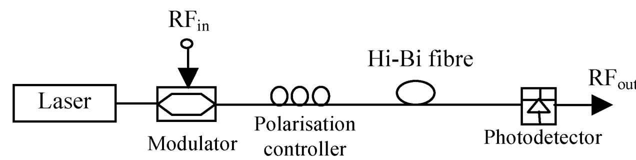


Fig. 20. Optical fiber delay-line filter using two linearly orthogonal polarized beams [62].

and a linearly chirped fiber grating is shown in Fig. 17 [58]. Such structures based on multiple wavelength sources also have versatile possibilities for realizing reconfigurable filter operation [58]. By changing the wavelength separation between the multiple wavelength sources, the basic delay time of the signal processor can be reconfigured and the filter center frequency can be programmed. Second, by changing the power of each wavelength source component, the time response of the filter can be apodized and, hence, the filter transfer function shape can be reconfigured.

In order to realize arbitrary high-resolution filters, it is essential to have the ability of generating both positive and negative polarity taps. This has been difficult to achieve in conventional photonic signal processors that operate through optical power manipulations and which consequently produce positive tap weights. An elegant solution to overcome this limitation is to use a dual-output Mach–Zehnder modulator to obtain outputs that have the RF signals modulated on the optical carriers in opposite phase, together with wavelength-selection gratings at each output. Using this concept, a single grating can be synthesized to realize the tap weights and delays simultaneously in one unit. Fig. 18 shows a structure that employs a grating synthesis technique that can realize both a flat-top filter and a high-rejection-ratio response simultaneously, while compressing the hardware requirements at the same time [59]. This enables taps to be readily obtained with short sampling times, together with bipolar taps using a dual-output electro-optic modulator.

The impulse response of a typical flat-top filter to be synthesized is shown in Fig. 19. Inverse scattering techniques can be employed to obtain both the mainlobe positive taps and the sidelobe negative taps with the requisite amplitudes and unit time delay intervals. The continuous layer peeling (CLP) technique [60] in conjunction with a windowing approach is applicable to synthesize the gratings that give the necessary reflectivity and group delay profile simultaneously, from which the requisite grating coupling coefficient is obtained.

The principal limitation of these WDM delay-line approaches is that each tap requires an individual laser source. The requirement for a large number of lasers with different wavelengths makes this approach difficult to implement for multitap high-resolution processors.

### *B. Photonic Signal Processor With Tap Polarization Control*

A second technique that can eliminate coherence limitations in photonic signal processors, and which has the advantage of requiring only a single laser source, is to use two orthogonal polarizations [61]. Two linearly orthogonal polarized beams in a fiber-optic system can be obtained using a high-birefringence (hi-bi) fiber where two linear polarization modes travel along the fast and slow axes, respectively, with a high extinction ratio [62]. Direct detection of the output optical power gives incoherent summing of the two optical signals. This technique is illustrated in Fig. 20 for a two-tap photonic filter.

An alternative implementation using birefringent crystals is shown in Fig. 21 [63]. This enables tunable operation to be obtained by changing the differential group delay by means of computer control.

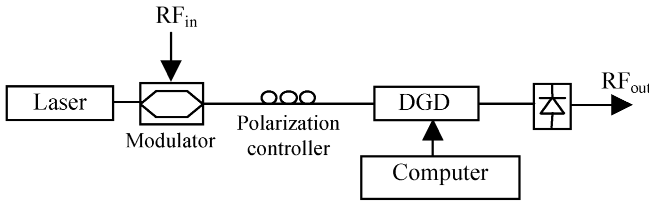


Fig. 21. Optical delay-line filter using two linearly orthogonal polarized beams implementated using birefringent crystals [63].

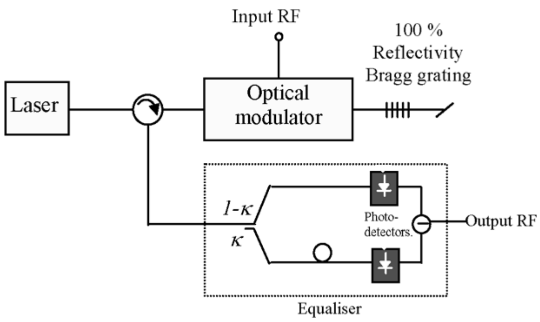


Fig. 22. Remodulation-based coherence-free photonic signal processor.

Microwave photonic filters using a variable polarization delay line can also be obtained using high-birefringence linear chirped gratings [64]. Tuning is possible by stretching or compressing the grating.

These techniques require very precise polarization control to ensure that correct polarization orientation is obtained and that the two polarization modes are equally excited and are generally suitable for realizing a limited number of taps.

### C. Remodulation-Based Photonic Signal Processors

A different technique for eliminating PIIN is shown in Fig. 22, with reference to a notch filter. The principle in this structure is to use remodulation of a single continuous wave carrier at different instants of times [65]. Light from a laser is modulated in a modulator in the forward direction and is then reflected back from a FBG to undergo a double-pass modulation in the modulator in the reverse direction. The second modulation produces notches at all frequencies where the remodulation is an odd integer multiple of 180° phase difference to the returned modulated RF signal. In this way, delayed samples of the RF signal are carried by the same optical signal and, thus, there is no optical interference in the photodetector. This precludes the deleterious effect of coherence.

The equalizer in Fig. 22 acts to widen the passband of the notch filter. The double-pass modulator output is split and fed into a two-arm delay-line filter structure with a balanced detection configuration. The two-arm delay-line filter has the same FSR as the double-pass modulation-based notch filter; however, the attenuation band of the two-arm delay-line filter is placed at the passband frequency of the double-pass modulation-based notch filter. By controlling the attenuation depth of the two-arm delay-line filter via the coupler coupling ratio, the overall response passband can be flattened. Only a shallow two-arm delay-line filter response is required to flatten the response of the double-pass modulation-based notch filter. Fig. 23 shows the response of the coherence-free wide-passband notch filter.

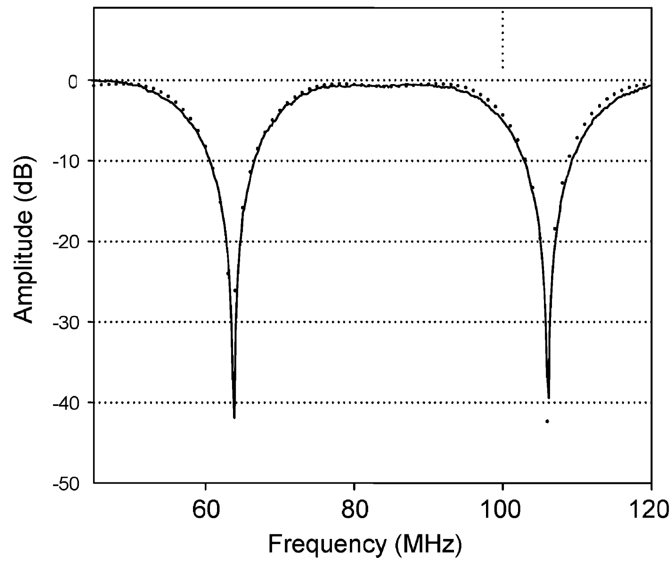


Fig. 23. Coherence-free wide-passband notch filter experimentally measured (solid line) and predicted (dotted line) response.

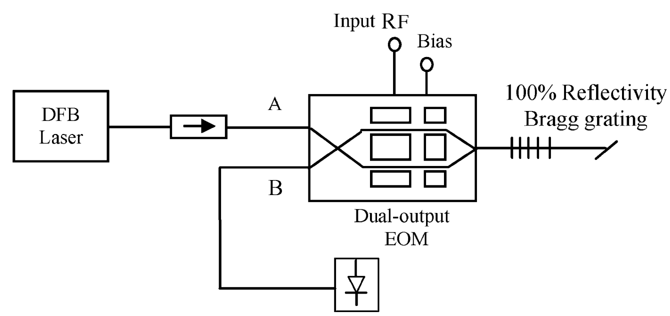


Fig. 24. Microwave photonic notch filter structure that realize negative taps without PIIN noise generation.

Since only a single optical path exists in the system prior to detection, there is no possibility of coherent interference effects. Since it is coherence-free, a narrow-linewidth laser source (such as a distributed feedback (DFB) laser) can be used to obtain a stable notch filter response. Also, there are no source-linewidth limitations to the high-frequency range of the filter operation; hence, only the modulator bandwidth determines this. Finally, and most importantly, no phase noise is generated in this structure. The attractiveness of this approach comprises its simplicity and ability to be built into an existing microwave fiber-optic link, since it only requires one additional fiber grating and a circulator beyond components that already exist in a fiber-optic link to provide filtering of unwanted RF signals.

The distance between the modulator and the grating reflection point controls the notch frequency of the filter. Hence, this structure can be extended to tunable notch operation by replacing the uniform Bragg grating with a chirped grating and by tuning the source wavelength. Tunable, narrow-linewidth laser sources are available and enable agile notch filter frequency tuning to be obtained.

An extension of this concept to realize negative taps without PIIN noise generation, is shown in Fig. 24 [66].

The structure is based on a reverse connection of a dual-output EOM and a grating reflector together with a remodulation technique. The modulated optical signal is reflected back from an FBG to undergo double-pass modulation in the modulator. The remodulated optical signals appear in both EOM output ports. The optical signal emerging from the EOM output port B has undergone a second modulation with the RF signal that has 180° phase difference to the first RF signal modulation and yields a two-tap negative-tap notch filter response. The distance between the modulator and the grating reflector controls the notch frequency.

These topologies eliminate the dominant PIIN. The remaining noise components at the output are the usual shot noise, laser intensity noise, and thermal noise, i.e., there is no additional noise generated by the signal processor. Since the output RF electrical power is proportional to the square of the input optical power and, among the noise components at the output, only the laser intensity noise is proportional to the square of the input optical power, it is possible to increase the SNR by increasing the input optical power until the system is laser intensity noise-limited. This is in contrast to conventional incoherent photonic notch filter structures, in which it is not possible to increase the SNR by increasing the input optical power because the phase noise is dominant for those structures and the phase noise increases with the square of the input optical power, just as the signal does. For example, over 60-dB increase in the SNR of the coherence-free notch filter has been measured, compared to the conventional unbalanced Mach–Zehnder delay-line notch filter, which uses incoherent summation of delayed signals [65]. Hence, this topology not only has a vastly lower intrinsic noise than conventional incoherent notch filter structures, but, unlike its counterpart, it enables even further improvement in noise to be realized by increasing the optical power, which is an important advantage.

### D. Sagnac-Based Photonic Signal Processors With High FSR

Photonic signal processors that are not only coherence-free, but which also achieve a high FSR and high-frequency operation, are of significant interest because wide-band operation is problematic using conventional electronic techniques.

A structure that can realize this, based on modulating a signal onto counterpropagating optical carriers, is illustrated in Fig. 25 [67]. This is based on a Sagnac fiber loop containing an off-loop-center optical modulator that modulates the clockwise (CW) and counterclockwise (CCW) propagating optical waves inside the Sagnac loop.

Using an intensity modulator in the loop that is located off center, the CW light and the CCW light are modulated by the same RF signal. The two modulated optical signals then travel through their remaining respective loop lengths before being recombined at the coupler. Since the CW and CCW light travel in the same transmission medium, any fluctuation in the loop length due to the changes in environmental conditions will affect the path length of the CW and CCW light equally. Hence, after recombination at the coupler, they will arrive at the photodetector at exactly the same time. Consequently, there is no coherent interference effect and there is no phase noise generation, as in conventional delay-line-based filters.

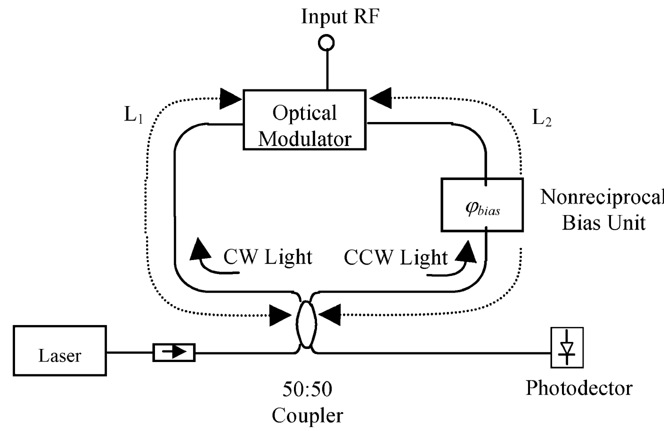


Fig. 25. Structure of the Sagnac-loop-based photonic notch filter topology.

Since the CW and CCW light propagating inside the loop travel different lengths after modulation occurs, the RF phases carried by the two modulated optical signals are different. After recombination, a notch filter response is produced when they are detected by the photodetector. The notches occur at frequencies where the RF phases of the two modulated optical signals are 180° different.

In this structure, the notch frequencies are determined by the fiber length difference $L_2 - L_1$, thus the FSR is inversely proportional to $L_2 - L_1$. This length difference can be made very small, hence this affords the opportunity of making the FSR very large and opens the way to realize notch filtering to very high microwave frequency, unlike conventional recirculating and linear delay-line structures that are limited by the minimum loop length rather than a difference in length.

### E. Multiple-Tap Coherence-Free Processors

The need to realize high-resolution, coherence-free photonic signal processors challenges current processor approaches in several ways. Many applications require high-frequency selectivity and high-$Q$ processors. This is difficult to realize for bandpass filters, because the achievement of high resolution in the frequency domain generically requires an increase in the number of taps in the impulse response of the discrete time signal processor. Previously reported photonic approaches to achieve a high-$Q$ and high-selectivity bandpass filters [18], [32] have involved splitting the light from the source, passing it through many different paths to obtain different delays, and then recombining them to sum. The fundamental problem with this approach is that the intrinsic phase randomness of the light source is inevitably converted into intensity fluctuation at the output, i.e., PIIN [37], [38]. As can be seen from the PIIN analysis in Section IV, this problem actually compounds as the number of taps is increased, since the PIIN generation at the photodetector increases due to the optical interference of the delayed signals, and this approach, in fact, cannot increase the $Q$ of the processor without also significantly increasing the deleterious PIIN, which is dominant.

We propose a new concept to solve the problem of simultaneously realizing both multiple-tap processor operation and with no PIIN generation for the first time. This is shown in Fig. 26.

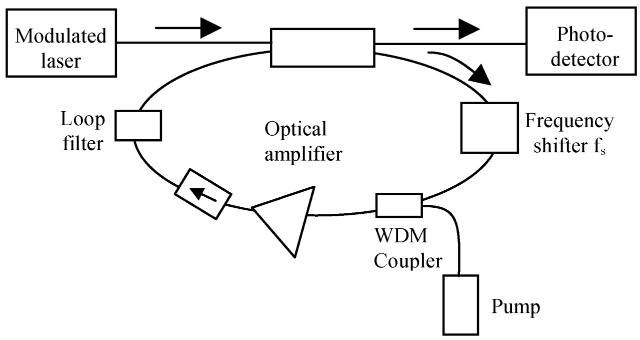


Fig. 26. Multiple-tap coherence-free processor.

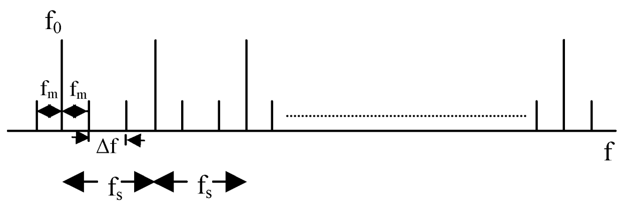


Fig. 27. Frequency shift needed in the loop to eliminate coherent interference effects.

The idea is to inject modulated light from a laser into a frequency-shifting loop. Each recirculation imposes a frequency shift $f_s$ on the light and produces a time delay $T$ and constitutes a tap in the impulse response. This new processor structure can create a large number of taps because numerous recirculations can occur, as they are ultimately limited only by the gain spectrum of the optical amplifier in the loop, which can be extremely large. However, the most significant innovation in this concept is that this method recombines signals at the photodetector at different wavelengths, so that the PIIN appears at the beat frequency corresponding to the frequency shift, instead of appearing at baseband, as is the case in conventional processors. Since this beat frequency is very high and falls outside of the bandwidth of the photodetector, the PIIN is automatically filtered out. This enables both a large number of taps to be generated and eliminates the dominant PIIN.

The frequency shift in the loop needs to satisfy certain conditions in order to eliminate coherent interference effects. This is shown in Fig. 27, which displays the intensity-modulated spectrum of the input laser at carrier frequency $f_0$ having RF modulation at frequency $f_m$, together with the generated frequency-shifted modulated carriers that are spaced at the frequency shifting value of $f_s$. If $f_s$ exceeds three times $f_m$, then the beating noise components at the photodetector fall outside the photodetector bandwidth and are filtered out.

The frequency shifter can be based on an electro-optic technique which can realize large frequency shifts [68] or a simple acousto-optic device. The optical amplifier functions to balance the optical losses occurring in the loop so that a large number of taps are evolved. An important advantage of this structure is that normal narrow-linewidth highly coherent telecommunications-type lasers can be used, instead of specially designed large-linewidth optical sources as in conventional approaches. The absence of PIIN results in SNR performance that is orders of magnitude higher than for conventional delay-line approaches. This new concept enables the realization of multiple-tap coherence-free processors that can operate without phase-noise limitations and which can generate a large number of taps and opens the way for realizing high-performance high-resolution photonic signal processors.

## IX. Conclusion

Photonic signal processing offers the possibility of realizing extremely high multigigahertz sampling frequencies, overcoming inherent electronic limitations. This stems from the intrinsic properties of optical delay lines that provide an excellent delay medium, due to its fundamental physical advantages of providing frequency-independent RF losses, very low and controllable dispersion, and frequency-independent RF signal multiplication/amplitude weighting. The reason for these key features arises because the RF fractional bandwidth is negligible for optical delay lines. In-fiber signal processors are inherently compatible with fiber-optic microwave systems. Hence, they can provide connectivity with built-in signal conditioning. This is especially useful in applications such as fiber-fed distributed antenna arrays, where the signal is already in the optical domain and enables RF preprocessing and filtering for signal conditioning while also providing EMI immunity. It can also provide unique solutions for realizing very wide-band octave and multioctave tunability, which is important for reconfigurable RF front-ends for radar systems.

Structures that can extend the performance of photonic signal processors have been presented. These include methods for improving the filter shape characteristics of microwave photonic filters to realize high-frequency selectivity in interference mitigation filters, techniques to obtain bandpass filters with high stopband attenuation and high skirt selectivity, and methods to realize operation with large FSR. A range of photonic signal processors, including high-resolution microwave filtering, widely tunable filters, arbitrary waveform generators, and fast and adaptive signal correlators, has been discussed. The importance of PIIN in photonic processors has been emphasized. Strategies that can solve this fundamental noise problem in photonic signal processors have been described. This includes coherence-free structures for few-tap notch filters, based on time-domain techniques. A new concept for realizing multiple-tap coherence-free processor filters based on a new frequency-shifting technique has also been presented. This structure not only eliminates the PIIN limitation, but can also generate a large number of taps to enable the realization of processors with high-frequency selectivity. These processors provide new capabilities for the realization of high-performance and high-resolution signal processing.

## Acknowledgment

The author would like to acknowledge the valuable contributions to this study of E. Chan, N. You, M. Shen, and J. Chen, all with the University of Sydney, Sydney, N.S.W., Australia.

## References

[1] K. Wilner and A. P. V. den Heuvel, “Fiber-optic delay lines for microwave signal processing,” *Proc. IEEE*, vol. 64, no. 5, pp. 805–807, May 1976.

[2] K. Jackson, S. Newton, B. Moslehi, M. Tur, C. C. Cutler, J. W. Goodman, and H. J. Shaw, "Optical fiber delay-line signal processing," *IEEE Trans. Microw. Theory Tech.*, vol. MTT-33, no. 3, pp. 193–204, Mar. 1985.

[3] M. Tur, J. W. Goodman, B. Moslehi, J. E. Bowers, and H. J. Shaw, "Fiber-optic signal processor with applications to matrix-vector multiplication and lattice filtering," *Opt. Lett.*, vol. 7, no. 9, pp. 463–465, 1982.

[4] S. A. Newton, R. S. Howland, K. P. Jackson, and H. J. Shaw, "High-speed pulse train generation using single-mode fiber recirculating delay lines," *Electron. Lett.*, vol. 19, pp. 756–758, 1983.

[5] B. Moslehi, J. W. Goodman, M. Tur, and H. J. Shaw, "Fiber-optic lattice signal processing," *Proc. IEEE*, vol. 72, no. 7, pp. 909–930, Jul. 1984.

[6] R. A. Minasian, "Photonic signal processing of high-speed signals using fiber gratings," *Opt. Fiber Technol.*, pp. 91–108, 2000.

[7] R. A. Minasian, K. E. Alameh, and E. H. W. Chan, "Photonics-based interference mitigation filters," *IEEE Trans. Microw. Theory Tech.*, vol. 49, no. 10, pp. 1894–1899, Oct. 2001.

[8] F. Coppinger, A. Bushan, and B. Jalali, "Photonic time stretch and its application to analog-to-digital conversion," *IEEE Trans. Microw. Theory Tech.*, vol. 47, no. 7, pp. 1309–1314, Jul. 1999.

[9] H. Roussell and R. Helkey, "Optical frequency conversion using a linearized LiNbO3 modulator," *IEEE Microw. Guided Wave Lett.*, vol. 8, no. 11, pp. 408–410, Nov. 1998.

[10] D. Hunter and R. Minasian, "Programmable high-speed optical code recognition using fiber Bragg grating arrays," *Electron. Lett.*, pp. 412–414, 1999.

[11] J. Chou, Y. Han, and B. Jalali, "Adaptive RF-photonic arbitrary waveform generator," *IEEE Photon. Technol. Lett.*, vol. 15, no. 4, pp. 581–583, Apr. 2003.

[12] H. Zmuda, R. Soref, P. Payson, S. Johns, and E. N. Toughlian, "Photonic beamformer for phased array antennas using fiber grating prism," *IEEE Photon. Technol. Lett.*, vol. 9, no. 2, pp. 241–243, Feb., 1997.

[13] P. Juodawlkis, J. Twitchell, G. Betts, J. Hargreaves, R. Younger, J. Wasserman, F. O'Donnell, K. Ray, and R. C. Williamson, "Optically sampled analog-to-digital converters," *IEEE Trans. Microw. Theory Tech.*, vol. 49, no. 10, pp. 1840–1853, Oct. 2001.

[14] Y. Han and B. Jalali, "Photonic time-stretched analog-to-digital converter: Fundamental concepts and practical considerations," *J. Lightw. Technol.*, vol. 21, no. 12, pp. 3085–3103, Dec. 2003.

[15] J. Capmany, B. Ortega, D. Pastor, and S. Sales, "Discrete-time optical processing of microwave signals," *J. Lightw. Technol.*, vol. 23, no. 2, pp. 702–723, Feb. 2005.

[16] A. Goutzoulis, "Photonic needs for phased array antennas," presented at the DARPA AOSP Workshop, 2000.

[17] E. Ackerman, C. Cox, J. Dreher, M. Davis, and D. DeBoer, "Fiber-optic antenna remoting for radio astronomy applications," in *Proc. URSI Gen. Assembly*, 2002, p. 65.

[18] B. Moslehi, "Fiber-optic filters employing optical amplifier to provide design flexibility," *Electron. Lett.*, vol. 28, no. 3, pp. 226–228, 1992.

[19] M. C. Vazquez, B. Vizoso, M. Lopez-Amo, and M. A. Muriel, "Single and double amplified recirculating delay lines as fiber-optic filters," *Electron. Lett.*, vol. 28, no. 11, pp. 1017–1019, 1992.

[20] B. Moslehi and J. W. Goodman, "Novel amplified fiber-optic recirculating delay line processor," *J. Lightw. Technol.*, vol. 10, no. 8, pp. 1142–1147, Aug. 1992.

[21] D. Norton, S. Johns, C. Keefer, and R. Soref, "Tunable microwave filtering using high dispersive fiber time delays," *IEEE Photon. Technol. Lett.*, vol. 6, no. 7, pp. 831–832, Jul. 1994.

[22] S. Sales, J. Capmany, J. Mart, and D. Pastor, "Solutions to the synthesis problem of optical delay line filters," *Opt. Lett.*, vol. 20, no. 23, pp. 2438–2340, 1995.

[23] M. Y. Frankel and R. D. Esman, "Fiber-optic tunable microwave transversal filter," *IEEE Photon. Technol. Lett.*, vol. 7, no. 2, pp. 191–193, Feb. 1995.

[24] J. Capmany, J. Cascon, J. L. Martin, S. Sales, D. Pastor, and J. Marti, "Synthesis of fiber-optic delay line filters," *J. Lightw. Technol.*, vol. 13, no. 10, pp. 2003–2012, Oct. 1995.

[25] T. Cusick, S. Iezekiel, M. Miles, S. Sales, and J. Capmany, "Synthesis of all-optical microwave filters using Mach–Zehnder lattices," *IEEE Trans. Microw. Theory Tech.*, vol. 45, no. 8, pp. 1458–1462, Aug. 1997.

[26] D. B. Hunter and R. A. Minasian, "Reflectivity tapped fiber-optic transversal filter using in-fiber Bragg gratings," *Electron. Lett.*, vol. 31, no. 12, pp. 1010–1012, 1995.

[27] F. Coppinger, S. Yegnanarayanan, P. D. Trinh, B. Jalali, and I. L. Newberg, "Nonrecursive tunable photonic filter using wavelength selective true-time-delay," *IEEE Photon. Technol. Lett.*, vol. 8, no. 9, pp. 1214–1216, Sep. 1996.

[28] F. Coppinger, S. Yegnanarayanan, P. D. Trinh, and B. Jalali, "Continuously tunable photonic radio-frequency notch filter," *IEEE Photon. Technol. Lett.*, vol. 9, no. 3, pp. 339–341, Mar. 1997.

[29] W. Zhang, J.A.R. Williams, L. A. Everall, and I. Bennion, "Fiber optic radio frequency notch filter with linear and continuous tuning by using a chirped fiber grating," *Electron. Lett.*, vol. 34, no. 18, pp. 1770–1772, 1998.

[30] T. A. Cusick, S. Iezekiel, and R. E. Miles, "All-optical microwave filter design employing a genetic algorithm," *IEEE Photon. Technol. Lett.*, vol. 10, no. 8, pp. 1156–1158, Aug. 1998.

[31] D. B. Hunter and R. A. Minasian, "Tunable microwave fiber-optic bandpass filters," *IEEE Photon. Technol. Lett.*, vol. 11, no. 7, pp. 874–876, Jul. 1999.

[32] N. You and R. Minasian, "A novel high-$Q$ optical microwave processor using hybrid delay-line filters," *IEEE Trans. Microw. Theory Tech.*, vol. 47, no. 7, pp. 1304–1308, Jul. 1999.

[33] ——, "High-$Q$ optical microwave filter," *Electron. Lett.*, vol. 35, no. 24, pp. 2125–2126, 1999.

[34] ——, "A novel tunable microwave optical notch filter," *IEEE Trans. Microw. Theory Tech.*, vol. 49, no. 10, pp. 2002–2005, Oct. 2001.

[35] W. Zhang and J.A.R. Williams, "Recirculating fiber-optic notch filter employing fiber gratings," *IEEE Photon. Technol. Lett.*, vol. 11, no. Jul., pp. 836–838, 1999.

[36] B. Vidal, V. Polo, J. L. Corral, and J. Marti, "Photonic microwave filter with tuning and reconfiguration capabilities using optical switches and dispersive media," *Electron. Lett.*, vol. 39, pp. 547–549, 2003.

[37] M. Tur, B. Moslehi, and J. Goodman, "Theory of laser phase noise in recirculating fiber-optic delay lines," *J. Lightw. Technol.*, vol. LT-3, no. 1, pp. 20–31, Jan. 1985.

[38] B. Moslehi, "Analysis of optical phase noise in fiber-optic systems employing a laser source with arbitrary coherence time," *J. Lightw. Technol.*, vol. LT-4, no. 9, pp. 1334–1351, Sep. 1986.

[39] J. Capmany, "Investigation on phase induced intensity noise in amplified fiber-optic recirculating delay line," *Electron. Lett.*, pp. 346–347, 1993.

[40] J. T. Kringlebotn and K. Blotekjaer, "Noise analysis of an amplified fiber-optic recirculating delay line," *J. Lightw. Technol.*, vol. 12, no. 3, pp. 573–581, Mar. 1994.

[41] H. Su, Y. Wang, F. Huang, and M. Lancaster, "Wide-band superconducting microstrip delay line," *IEEE Trans. Microw. Theory Tech.*, vol. 52, no. 11, pp. 2482–2487, Nov. 2004.

[42] A. Molony, L. Zhang, J.A.R. Williams, I. Bennion, C. Edge, and J. Fells, "Fiber Bragg-grating true time-delay systems: Discrete-grating array 3-b delay lines and chirped-grating 6-b delay lines," *IEEE Trans. Microw. Theory Tech.*, vol. 45, no. 8, pp. 1527–1530, Aug. 1997.

[43] M. Shen and R. A. Minasian, "Linearization processing of a novel short time-delay WDM superposed fiber Bragg grating," *IEEE Photon. Technol. Lett.*, vol. 14, no. 12, pp. 1707–1709, Dec. 2002.

[44] A. Pothier, "Low-loss 2-bit tunable bandpass filter using MEM's DC contact switches," *IEEE Trans. Microw. Theory Tech.*, vol. 53, no. 1, pp. 354–360, Jan. 2005.

[45] K. Entesari and G. Rebeiz, "A differential 4-bit 6.5–10 GHz RF MEMS tunable filter," *IEEE Trans. Microw. Theory Tech.*, vol. 53, no. 3, pp. 1103–1110, 2004.

[46] A. Papoulis, *Probability, Random Variables, and Stochastic Processes*. New York: McGraw-Hill, 1965.

[47] M. Tur and A. Arie, "Phase induced intensity noise in concatenated fiber-optic delay lines," *J. Lightw. Technol.*, vol. 6, no. 1, pp. 120–130, Jan. 1988.

[48] P. Pepeljokowski and K. Lau, "Interferometric noise reduction in fiber-optic links by superposition of high frequency modulation," *J. Lightw. Technol.*, vol. 10, no. 7, pp. 957–963, Jul. 1992.

[49] I. T. Monroy, E. Tangdiongga, R. Jonker, and H. de Waardt, "Interferometric crosstalk reduction by phase scrambling," *J. Lightw. Technol.*, vol. 18, no. 5, pp. 637–646, May 2000.

[50] E. H. W. Chan, K. E. Alameh, and R. A. Minasian, "Photonic bandpass filters with high skirt selectivity and stopband attenuation," *J. Lightw. Technol.*, vol. 20, no. 11, pp. 1962–1967, Nov. 2002.

[51] B. Vidal, V. Polo, J. Corral, and J. Marti, "Harmonic suppressed photonic microwave filter," *J. Lightw. Technol.*, vol. 20, no. 12, pp. 3150–3154, Dec. 2003.

[52] E. H. W. Chan and R. A. Minasian, "High-resolution photonics-based interference suppression filter with wide passband," *J. Lightw. Technol.*, vol. 21, no. 12, pp. 3144–3149, Dec. 2003.

[53] J. Chou, Y. Han, and B. Jalali, "Adaptive RF-photonic arbitrary waveform generator," *IEEE Photon. Technol. Lett.*, vol. 15, no. 4, pp. 581–583, Apr. 2003.

[54] M. Hyodo, K. S. Abedin, and N. Onodera, "Generation of arbitrary optical waveforms by Fourier synthesis using three continuous-wave semiconductor lasers," *Electron. Lett.*, pp. 224–225, 2000.
[55] M. Shen and R. A. Minasian, "High-speed arbitrary waveform generation by a novel photonic processing structure," *IEEE Photon. Technol. Lett.*, vol. 16, no. 4, pp. 1155–1157, Apr. 2004.
[56] D. Hunter and R. Minasian, "Programmable high-speed optical code recognition using fiber Bragg grating arrays," *Electron. Lett.*, vol. 35, no. 5, pp. 412–414, 1999.
[57] N. You and R. A. Minasian, "Grating-based optical microwave FIR filter," in *Proc. Eur. Microw. Conf.*, vol. 2, Paris, France, 2000, pp. 49–51.
[58] J. Capmany, D. Pastor, and B. Ortega, "New and flexible fiber-optic delay-line filters using linearly chirped Bragg gratings and laser arrays," *IEEE Trans. Microw. Theory Tech.*, vol. 47, no. 7, pp. 1321–1326, Jul. 1999.
[59] J. L. Chen and R. A. Minasian, "Novel synthesised photonic signal processor with hardware compression," *IEEE Photon. Technol. Lett.*, vol. 17, no. 4, pp. 896–898, Apr. 2005.
[60] J. Skaar, L. Wang, and T. Erdogan, "On the synthesis of fiber Bragg gratings by layer peeling," *IEEE J. Quantum Electron.*, vol. 37, no. 1, pp. 165–173, Jan. 2001.
[61] A. Arie and M. Tur, "The effects of polarization control on the transfer function and the phase induced intensity noise of a fiber-optic recirculating delay line," *J. Lightw. Technol.*, vol. 6, no. 10, pp. 1566–1574, Oct. 1988.
[62] W. Zhang, J. A. R. Williams, and I. Bennion, "Optical fiber delay line filter free of the limitation imposed by optical coherence," *Electron. Lett.*, vol. 35, no. 24, pp. 2133–2134, 1999.
[63] J. Chen, Y. Wu, J. Hodiak, and P. Yu, "A novel digitally tunable microwave-photonic notch filter using differential group-delay module," *IEEE Photon. Technol. Lett.*, vol. 15, no. 2, pp. 284–286, Feb. 2003.
[64] X. Yi, C. Lu, X. Yang, W. Zhong, F. Wei, L. Ding, and Y. Wang, "Continuously tunable microwave-photonic filter design using high-birefringence linear chirped grating," *IEEE Photon. Technol. Lett.*, vol. 15, no. 5, pp. 754–756, May 2003.
[65] E. H. W. Chan and R. A. Minasian, "Photonic notch filter without optical coherence limitations," *J. Lightw. Technol.*, vol. 22, no. 7, pp. 1811–1817, Jul. 2004.
[66] ——, "Novel all-optical RF notch Filters with equivalent negative tap response," *IEEE Photon. Technol. Lett.*, vol. 16, no. 5, pp. 1370–1372, May 2004.
[67] ——, "Coherence-free photonic notch filter," *Electron. Lett.*, vol. 40, no. 21, pp. 1375–1377, 2004.
[68] S. Shimotsu, S. Oikawa, T. Saitou, N. Mitsugi, K. Kubodera, T. Kawanishi, and M. Izutsu, "Single side-band modulation performance of a $LiNbO_3$ integrated modulator consisting of four-phase modulator waveguides," *IEEE Photon. Technol. Lett.*, vol. 12, no. 4, pp. 364–366, Apr. 2001.

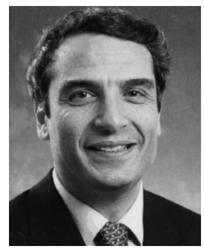

**Robert A. Minasian** (S'78–M'80–SM'00–F'03) received the B.E. degree from the University of Melbourne, Melbourne, Australia, the M.Sc. degree from the University of London, University College, London, U.K., and the Ph.D. degree from the University of Melbourne.

He is currently a Professor and holds a Personal Chair with the School of Electrical and Information Engineering, University of Sydney, Sydney, Australia, and is Director of the Fiber-Optics and Photonics Laboratory. His research encompasses optical telecommunications and signal processing and currently centers on photonic signal processing, broad-band optical communications, microwave photonics, and optical phased arrays. He has contributed 200 technical publications in these areas. He is an Associate Editor of *Optical Fiber Technology*.

Prof. Minasian is a Fellow of the Institute of Engineers, Australia. He serves on the Australian Research Council as a member of the College of Experts. He is a member of the Technical Committee on Microwave Photonics of the IEEE Microwave Theory and Techniques Society (IEEE MTT-S) and has served and is on the Program Committees for several international conferences including the IEEE International Meeting on Microwave Photonics, (MWP2000, MWP2003, MWP2006), the Asia–Pacific Microwave Conference (APMC 2000), the IEEE MTT-S International Microwave Symposium (IMS2006), and the IEEE Lasers and Electro-Optics Society (IEEE LEOS) Annual Meeting (LEOS2005). He was the recipient of the ATERB Medal for Outstanding Investigator in Telecommunications awarded by the Australian Telecommunications and Electronics Research Board.